ACS APPLIED MATERIALS & INTERFACES

Research Article

Cite This: ACS Appl. Mater. Interfaces 2019, 11, 48564−48573

www.acsami.org

Supramolecular Fabrication of Complex 3D Hollow Polymeric Hydrogels with Shape and Function Diversity

Baoyi Wu,[†,‡] Yukun Jian,[†,§] Xiaoxia Le,[†,§] Han Lin,[†] Shuxin Wei,[†,§] Wei Lu,[†,§] Jiawei Zhang,[*,†,§] Afang Zhang,[‡] Chih-Feng Huang,[∥] and Tao Chen[*,†,§]

[†]Key Laboratory of Marine Materials and Related Technologies, Zhejiang Key Laboratory of Marine Materials and Protective Technologies, Ningbo Institute of Material Technology and Engineering, Chinese Academy of Sciences, Ningbo 315201, China

[‡]Department of Polymer Materials, College of Materials Science and Engineering, Shanghai University, Nanchen Road 333, Shanghai 200444, China

[§]School of Chemical Sciences, University of Chinese Academy of Sciences, 19A Yuquan Road, Beijing 100049, China

[∥]Department of Chemical Engineering, National Chung Hsing University, 145 Xingda Road, Taichung 402-27, Taiwan

Supporting Information

ABSTRACT: Inspired by the high importance of hollow structures in nature such as blood vessels and bamboos in matter transportation, properties enhancement, or even survival of living creatures, the creation of hollow materials remains of considerable interest. However, constructing hollow unique living-like soft and wet polymeric hydrogels with desirable structures and functionalities is still a big challenge. Here, we reported a robust and effective strategy to fabricate complex three-dimensional (3D) hollow polymeric hydrogel with designed shape and function diversity on the basis of supramolecular interactions. By placing a Ca^{2+} included gelatin core into the solution of alginate, hydrogel shell could be formed along with the shape of the gelatin core via coordination between alginate chains and Ca^{2+} diffused from gelatin. The hollow hydrogel could finally be obtained by dissolving the gelatin core. Various complex 3D hollow structures could be achieved by designing/constructing assembled gelatin core as a building block with adjustable supramolecular metal coordination position and strength. Moreover, hollow hydrogels with function diversity could be developed by introducing functional polymers or nanoparticles into the hydrogel wall. This work has made important progress in developing hollow polymeric hydrogel with desirable structures, shapes, and various functional applications including soft actuators and chemical reaction containers.

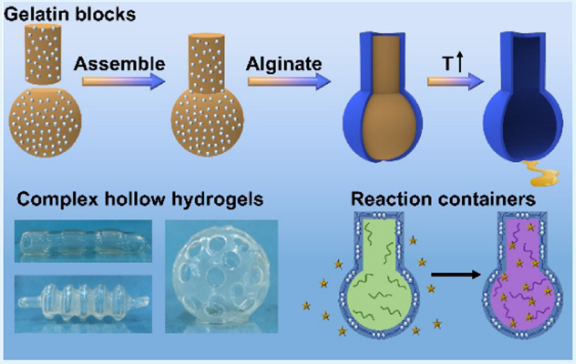

KEYWORDS: *3D hollow hydrogels, supramolecular interaction, pneumatic/hydraulic actuators, material transportation, functional reaction containers*

1. INTRODUCTION

The wide presence of the hollow structures in nature, such as blood vessels and the stems of bamboo, reeds etc, is crucial to the survival of the living creatures owing to their extraordinary characteristics such as material transport capacity, mechanical properties enhancement, and so on. Nature has provided us the abundant inspiration for the design of novel materials.[1−6] In particular, as soft and wet with living-like properties, polymeric hydrogels,[7−11] have attracted increasing attention in bioinspired materials design and applications.[12−21] However, there are only a limited number of examples that polymeric hydrogels have used to fabricate hollow structures, which is probably because hydrogels are not easy to be manufactured due to the soft and wet nature. There are preliminary attempts to fabricate hollow hydrogels. In the current stage, there are a few strategies to construct hydrogels with hollow structures,[22−31] three-dimensional (3D) printing, and removal of sacrificial materials. For instance, Zhao et al. and Qu et al. have presented hollow hydrogel cubes via 3D printing, respectively.[25,26] However, their strategies require a professional 3D printer with high resolution and only limited materials can be used as inks. Few efforts have been devoted to fabricate hollow hydrogels through removing templates, alternatively.[29−31] For instance, Zhou et al. have proposed an effective method to prepare hollow hydrogels by on-site surface radical polymerization using high-purity iron wire as an initiation template.[30,31] However, their approach could only achieve hollow structures with large openings, and the applications are limited. At present, constructing hollow, soft, and wet polymeric hydrogels with desirable structures and functions remains a significant challenge.

Received: September 25, 2019
Accepted: November 19, 2019
Published: November 19, 2019

DOI: 10.1021/acsami.9b17440
ACS Appl. Mater. Interfaces 2019, 11, 48564−48573

Scheme 1. (a) Images Show the Hollow Structure of Bamboo and Gourd[a]

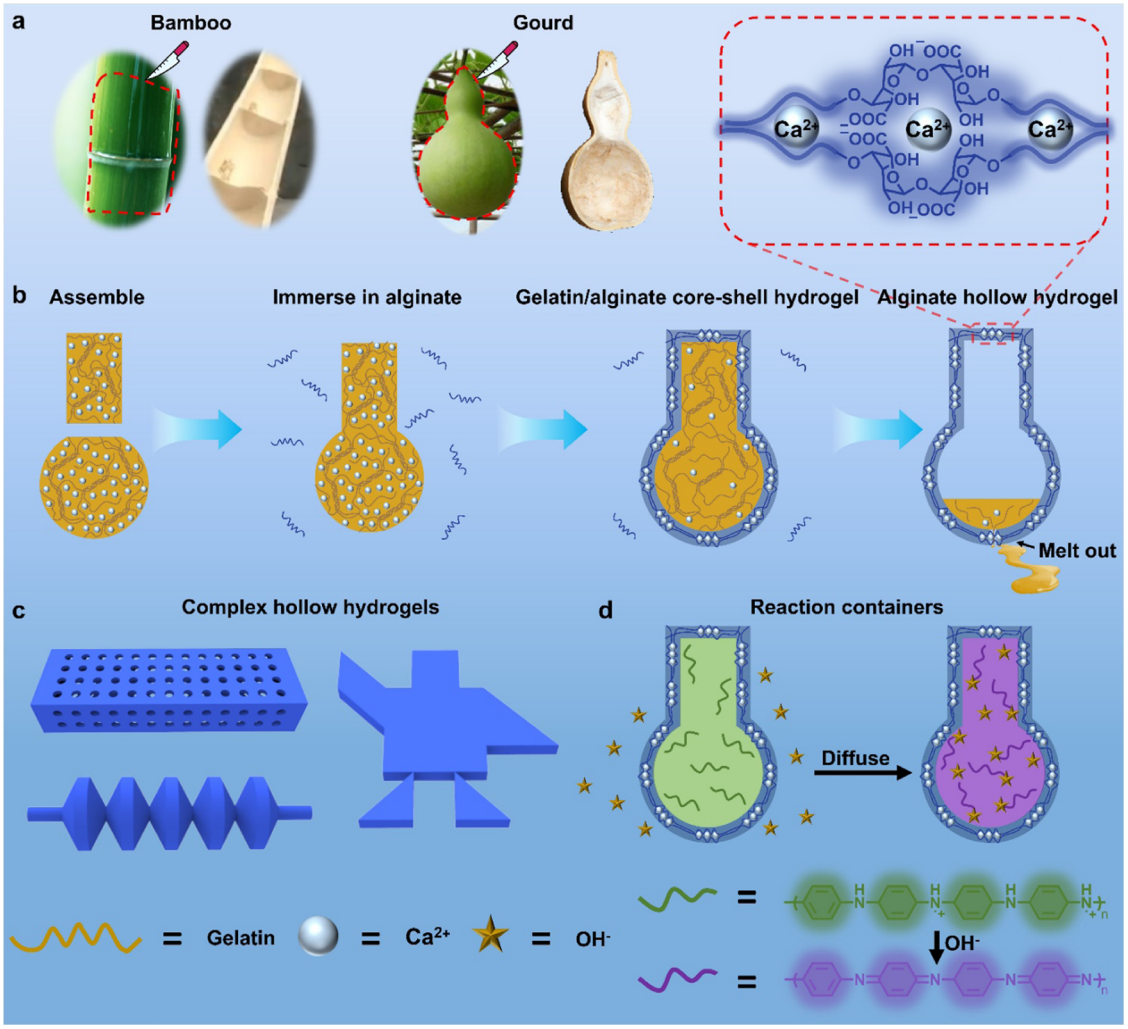

[a](b) Schematic illustration of the supramolecular preparation of hollow hydrogels. The assembled gelatin core is immersed into the solution of alginate, gelatin/alginate core−shell hydrogel is formed by Ca^{2+}−alginate coordination, finally hollow hydrogel is obtained after the gelatin melted and flowed out from the pre-punched hole. (c) Various complex hollow hydrogels could be achieved through using assembled gelatin cores or controlling the diffusion position of Ca^{2+}. (d) Schematic illustration of the hollow hydrogel as a chemical reactor where the small molecule (OH^-) can diffuse into the reactor and react with polyaniline (PANI).

Supramolecular interactions have been widely applied to construct soft materials.[32−37] In our previous work, we have also fabricated various smart polymeric hydrogels for the application of self-healing, shape memory, and actuating based on supramolecular interactions.[38−45] In particular, gelatin that could form a hydrogel in cold environment and melt in warm temperature has been employed to develop smart polymeric hydrogels.[46]

Inspired by the hollow structure of natural plants such as bamboo and gourd (Scheme 1a), herein, we present an effective approach for constructing complex three-dimensional (3D) hollow hydrogel with shape and function diversity. A gelatin core containing $CaCl_2$ was first assembled from small gelatin blocks, then the gelatin core was transferred into a solution of sodium alginate, and an alginate-based hydrogel shell could be generated along with the shape of gelatin core through supramolecular interactions between alginate chains and Ca^{2+} diffused from gelatin (Scheme 1b). The gelatin/alginate core−shell hydrogel was treated by warm water to induce the melting of gelatin core, and various 3D hollow hydrogels with shape diversity could finally be achieved by using assembled gelatin cores or controlling the metal coordination position and strength (Scheme 1c). The obtained hollow hydrogels could be applied as pneumatic/hydraulic actuators. Moreover, the hollow hydrogels could be considered as an ideal candidate as chemical reactors with regulated speed since the hydrogel walls could allow small molecules to pass through (Scheme 1d). In addition, functional hollow hydrogels could be accomplished by integrating functional polymer or nanoparticles (NPs) into the hydrogel wall. Our strategy may promote the development of novel complex hollow polymeric hydrogel systems with various applications such as soft actuators and chemical reaction containers.

2. EXPERIMENTAL SECTION

2.1. Materials. Gelatin, aniline (ANI, ≥99.0%), sodium dodecyl sulfate (SDS, ≥99.0%), ammonium persulfate(APS, ≥98.0%), methyl violet, ethylenediaminetetraacetic acid (EDTA), brilliant blue, tartrazine, methyl blue, Evans blue, fluorescein, calcium chloride ($CaCl_2$), copper chloride ($CuCl_2$), magnesium chloride ($MgCl_2$), ferric chloride ($FeCl_3$), aluminum chloride ($AlCl_3$), calcium sulfate

DOI: 10.1021/acsami.9b17440
ACS Appl. Mater. Interfaces 2019, 11, 48564−48573

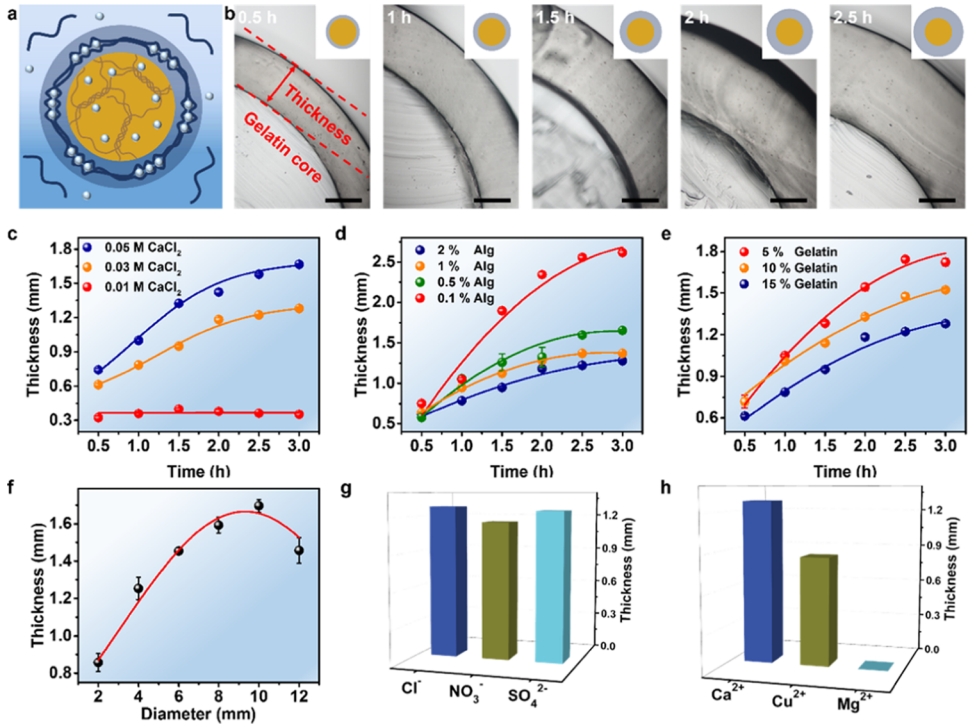

Figure 1. (a) Illustration of a cylindrical gelatin-alginate core−shell hydrogel. (b) Images showing the process of hydrogel growth. (c) The dependence of the hydrogel thickness with different concentrations of $CaCl_2$ as a function of growth time. (d) The dependence of the hydrogel thickness with different concentrations of alginate as a function of growth time. (e) The dependence of the hydrogel thickness with different concentrations of gelatin as a function of growth time. (f) The dependence of the hydrogel thickness with different diameter of gelatin core. (g) The effect of anions on hydrogel thickness. (h) The effect of cations on hydrogel thickness. Scale bar: 0.5 mm.

($CaSO_4$), calcium nitrate ($Ca(NO_3)_2$), *p*-nitrophenol, and sodium borohydride were purchased from Aladdin Chemistry Co. Ltd. Gold(III) chloride trihydrate ($HAuCl_4 \cdot 3H_2O$, 99.9%), tris-(hydroxymethyl) aminomethane, and dopamine hydrochloride were purchased from Sigma-Aldrich. Sodium alginate (Alg) was purchased from Sinopharm Chemical Reagent Co. Ltd. Clone power (L-61212) was purchased from SIRWHISTON.

2.2. Instruments. Steady-state fluorescence spectra were measured on a Hitachi F-4600 spectrofluorometer at controlled conditions equipped with a Xenon (Xe) lamp (150 W). Scanning electronic microscopy (SEM) measurements were characterized by a Hitachi S4800 microscope. UV−vis absorption spectra were recorded by virtue of TU-1810 UV−vis spectrophotometer provided by Purkinje General Instrument Co. Ltd. The image of tubular hydrogels was taken by a polarizing microscope (OLYMPUS, 71781687-5).

2.3. Preparation of Tubular Hydrogel. Gelatin (15 g) and 555 mg $CaCl_2$ were dissolved in 100 mL deionized water at 60 °C. Then the solution was transferred into tubular molds. After gelation at 4 °C for 30 min, the gelatin was obtained after removing the mold. Then the obtained gelatin core was immersed into the solution of alginate (2 wt %). After 1 h, the tubular hydrogels were obtained after transferring the gelatin/alginate hydrogel into warm water to remove the gelatin core.

2.4. Preparation of 3D Gelatin Core. The 3D gelatin was fabricated by the traditional mold-making process. At first, a mold of poly(lactic acid) (PLA) was prepared by a traditional 3D printer. Then it was immersed into the solution of clone powder, which is prepared by mixing the cloned powder with water in a ratio of 1:5. After 20 min, the PLA model was removed from the gelled clone. At last, a solution of gelatin (15 wt %) containing $CaCl_2$ (0.05 M) was injected into the cavity of the cloning gel, then the 3D gelatin hydrogel was obtained by breaking the model down.

2.5. Preparation of Complex Hollow Hydrogel. The complex gelatin core was prepared as mentioned above and immersed into the solution of alginate (2 wt %). After 1 h, the gelatin/alginate hydrogel was transferred into the solution of $CaCl_2$ and then the complex hollow hydrogels were obtained after transferring the gelatin/alginate hydrogel into hot water to remove the gelatin core.

2.6. Synthesis of PANI. A mixture of aniline (4 μL, 0.02 mM) and SDS (5 mL, 0.2 mM) was prepared, then the resultant solution was mixed with an acidic $(NH_4)_2S_2O_8$ solution (30 mL 0.06 mM in 10 mM HCl). Finally, the solution was incubated at room temperature for 24 h.

2.7. Preparation of Alginate/PANI Hydrogel. Alginate (700 mg) was dissolved into a 35 mL PANI solution. A gelatin core containing $CaCl_2$ (0.05 M) was immersed into the alginate/PANI solution. After 1 h, the alginate/PANI tubular hydrogels were obtained after transferring the gelatin/alginate/PANI hydrogel into hot water to remove the gelatin core.

2.8. Preparation of Alginate/Polydopamine (PDA)/AuNPs Hydrogel. A 5 mL of dopamine aqueous solution (2 mg/mL) was poured into the prepared tubular hydrogel. Then, 0.5 mL of tris−HCl buffer solution (0.1 M, pH = 8.5) was dropped into the above dopamine solution. The resultant mixed solution gradually changed to brown color. After 2 h, the dopamine solution was poured off and 5 mL of $HAuCl_4$ solution (2.5 mM) was added. After 2 h, the alginate/PDA/AuNPs hydrogel was obtained after removing the $HAuCl_4$ solution.

2.9. Experiment of Molecules Exchange. The tubular hydrogel with one end open was prepared as mentioned above, 3 mL of dye molecule (Methyl violet, brilliant blue, Tartrazine, Methyl blue, Evans blue, Fluorescein, 1.87 mM) was injected into the tubular hydrogel. Then, the tubular hydrogel was placed in a glass square cylinder containing 80 mL deionized water. A 3 mL solution was taken from the glass square cylinder every hour for ultraviolet-visible light analysis. (The removed solution should be returned to keep the total amount of water in the container same.)

DOI: 10.1021/acsami.9b17440
ACS Appl. Mater. Interfaces 2019, 11, 48564−48573

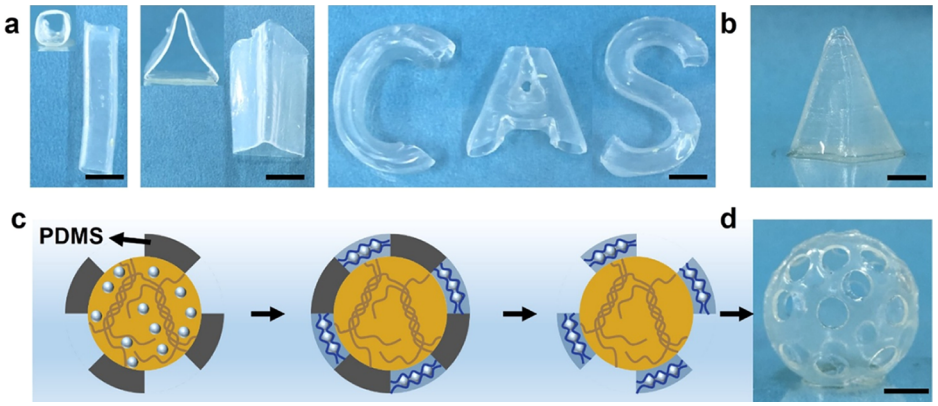

Figure 2. (a) Images of hollow hydrogels such as tubes with different cross-sectional shapes (squares, triangles) and hollow English letters. (b) Image of 3D complex hollow hydrogel. (c) Illustration showing the preparation of hollow hydrogel with macroporous structure. (d) Image of hollow hydrogel with macroporous structure. Scale bar: 1 cm.

3. RESULTS AND DISCUSSION

The hollow hydrogels were fabricated by diffusion-induced gelation from the inside out, and the process of growth can be visualized from the optical images. A cylindrical gelatin core containing 0.03 M $CaCl_2$ was placed in the solution of alginate (2 wt %), a uniform alginate hydrogel layer was formed as the shell as Ca^{2+} diffused from the gelatin core and crosslinked the alginate chains (Figure 1a). The cylindrical gelatin-alginate hydrogel was investigated after slicing every 0.5 h, the gelatin core and alginate hydrogel wall can be obviously observed from the images, and the wall slowly thickens as time progresses (Figure 1b). Since the growth of the alginate hydrogel is dependent on the diffusion of Ca^{2+}, it can be speculated that the factors that affect the diffusion of Ca^{2+} also affect the kinetics of growth such as the concentrations of Ca^{2+}, alginate, and gelation. As the concentration of Ca^{2+} increases, the thickness of the wall shows a faster increase (Figures 1c and S1−3). While the thickness of the wall decreases with increasing concentrations of alginate and gelatin, which indicates that the dense alginate and gelatin chains will hinder the diffusion of Ca^{2+} (Figures 1d,e and S4−5). Moreover, the influence of the diameter of cylindrical gelation core was also evaluated, as the diameter of gelatin core increases, the thickness of the wall shows a tendency to decrease after increasing to the highest value (Figure 1f). The microstructure of the alginate hydrogel was investigated by scanning electron microscopy (SEM). As shown in Figure S6, the alginate layer exhibits denser porous structures with increasing content of alginate. In addition, various cations such as Mg^{2+}, Cu^{2+}, Fe^{3+}, and Al^{3+} and anions such as Cl^-, NO_3^-, and SO_4^{2-} were respectively mixed into the gelatin core in the concentration of 0.03 M. As shown in Figures 1g and S7, the thickness of hydrogels grown with Ca^{2+} are hardly affected by anions. While cations have a significant influence on the thickness of the alginate layer, the hydrogel grown with Cu^{2+} is thinner than that grow with Ca^{2+}, and hydrogel cannot be generated if Mg^{2+} is incorporated (Figure 1h). Unfortunately, due to the strong coordination between Fe^{3+} and Al^{3+} with gelation, the obtained gelatin hydrogel cannot be molded. These results indicate that the formation of the alginate layer is related to the binding capacity between the cations with alginate and gelatin. Cations with strong coordination with gelatin are not easy to be diffused out, while those which cannot be effectively combined with alginate will form a thin hydrogel layer, therefore cations should be chosen to realize an optimize performance. The results show that the thickness of the alginate layer could be tuned by many factors, it could be anticipated that hollow hydrogel structures with both large and small sizes could be obtained by adjusting the operating circumstances.

Hollow alginate hydrogel tubes could be obtained if the gelatin core is dissolved in warm water, and 3D hollow hydrogels can be fabricated if a 3D gelatin core is used. Briefly, a 3D model of PLA was obtained by 3D printing, then a 3D gelatin core was achieved by replicating the PLA model (Scheme S1). Finally, a lot of complex 3D hollow hydrogels could be developed by dissolving the gelatin core, such as the tubes with different cross-sectional shapes (squares, triangles, hollow English letters, and Chinese characters (Figures 2a and S8a)). Furthermore, hollow structures like traditional buildings such as Colosseum and Pyramid can be also achieved (Figures 2b and S8b). Using the process of Ca^{2+} diffusion, not only results in a closed shell structure that is completely consistent with the core but also the growth process can be easily controlled to prepare a more interesting shell structure. Some poly(dimethylsiloxane) (PDMS) flakes were attached to the surface of the gelatin core since PDMS will prevent the diffusion of Ca^{2+}, a hollow hydrogel with macroporous structure is further obtained (Figures 2c,d and S8c).

Hollow alginate hydrogel tubes could be obtained if the gelatin core is dissolved in warm water, and the stiffness of the hydrogel tubes could be tuned by Ca^{2+}. The as-prepared hydrogel tubes are soft and cannot support its own weight, while with the introduction of extra Ca^{2+}, more alginate−Ca^{2+} crosslinks will be formed and the tube will become more stiffer, and tube will turn to soft again if some Ca^{2+} is extracted by ethylenediaminetetraacetic acid (EDTA) (Figure S9). Besides, the stiffness of alginate hydrogels was also measured (Figure S10), the tensile stress of the hydrogel wall increases with increasing treatment time with Ca^{2+}. Due to the modulus adjustable capacity, the 3D alginate hollow hydrogel exhibits shape memory property. As shown in Figure S11, a macroporous hollow hydrogel was squashed and immersed in the solution of $CaCl_2$ (0.1 M) for 10 min, the temporary shape can be fixed, and it will recover when treated with ethylenediaminetetraacetic acid (EDTA, 0.1 M). The hollow hydrogel could also be applied as containers (Figure S12). Some pieces of gelatin loaded with Cu^{2+} was placed inside the macroporous hollow hydrogel, the gelatin will be well preserved at ambient temperature, and they will diffuse

DOI: 10.1021/acsami.9b17440
ACS Appl. Mater. Interfaces 2019, 11, 48564−48573

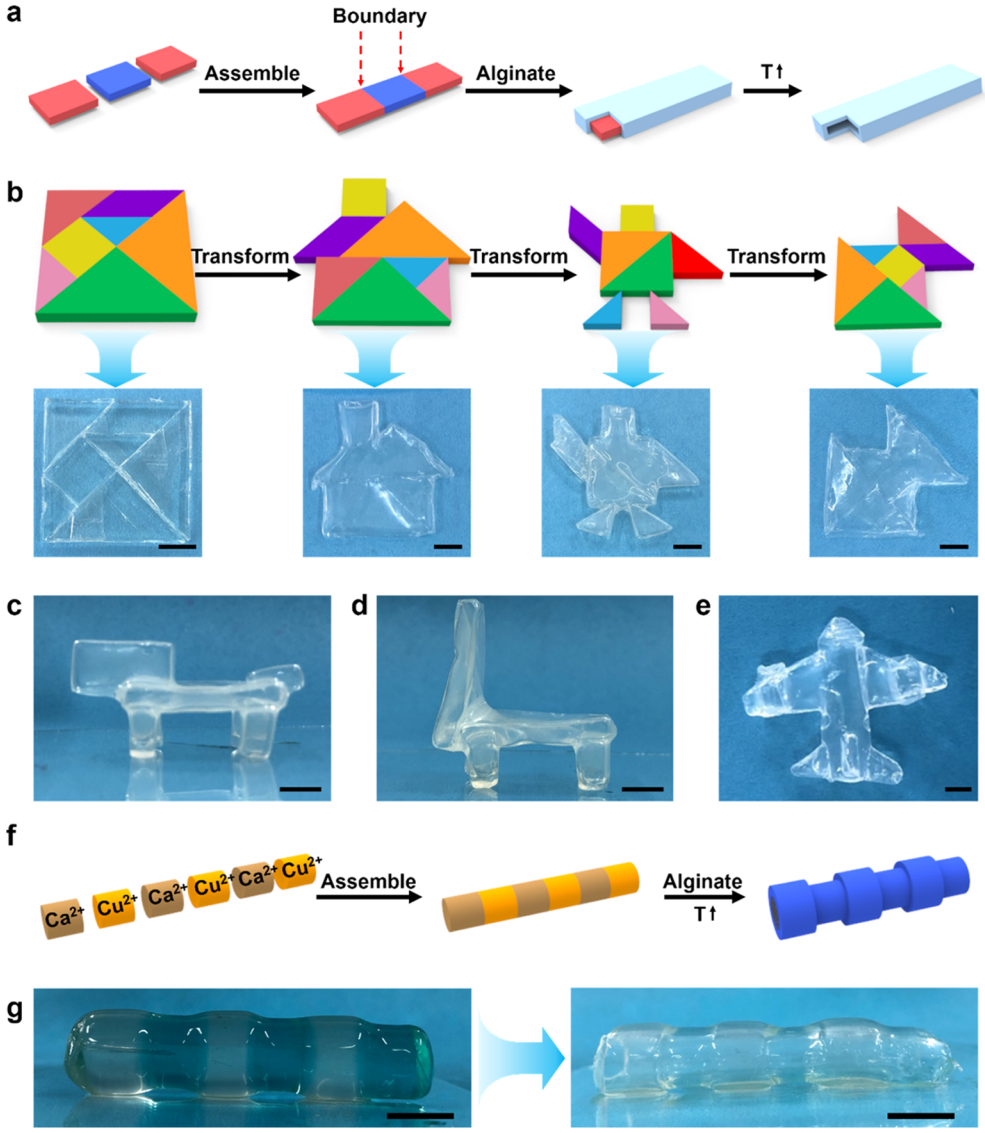

Figure 3. (a) Illustration showing the preparation of hollow hydrogel by the assembly of gelatin cores. (b) Illustration showing the assembly process of tangram (from the shape of a square to the shapes of house, human, and fish), and images showing the complex hollow hydrogels. (c−e) Images showing the complex 3D hollow hydrogels through assembled 3D gelatin cores. (f, g) Illustration and images showing the preparation of tubular hydrogel with uneven surface. Scale bar: 1 cm.

through the holes to outside if the temperature rises to 50 °C (Movie S1).

Through assembling gelatin blocks with simple shapes, hollow alginate hydrogels with more complex shapes could be accomplished. As shown in Figure 3a, three pieces of gelatin blocks are assembled together and then immersed into the solution of alginate. Although the assembled gelatin core has obvious boundaries, the alginate hollow hydrogel after growth will be intact. Inspired by the tangram, seven pieces of gelatin blocks with the same shape of the tangram have been prepared. Through assembling, a variety of two-dimensional (2D) gelatin cores such as a house, human, and fish were obtained (Figures 3b and S13), then the corresponding hollow hydrogels were fabricated. The hollow hydrogel could be expanded when inhaling (Movies S2−4), indicating they have a closed hollow structure and good mechanical properties. Besides, 3D hollow hydrogel such as dog, chair can be also obtained through assembled 3D gelatin cores (Figures 3c,d and S14−15). Combining 3D printing technology with the assembly of gelatin blocks, the more complex 3D model could be obtained. As shown in Figure 3e, the fuselage, wings, and engine of an aircraft were constructed by gelatin, then these parts were assembled to the correct position (Figure S16). The hollow alginate hydrogel aircraft was obtained after hydrogel growth and enucleated. Subsequently, three pieces of gelatin loaded with Ca^{2+} and three pieces of gelatin loaded with Cu^{2+} were assembled (Figure 3f), because the alginate layer formed by the diffusion of Ca^{2+} is thicker than that formed by the diffusion of Cu^{2+}, the tubular hydrogel with a smooth inner wall but an uneven outer wall is obtained (Figure 3g). It could be assumed that if the obtained 3D hollow hydrogels are treated by Ca^{2+} and then immersed into alginate solution, the multilayered 3D hollow system could be achieved. Not only alginate but other polymers that are able to crosslink by metal ions such as chitosan are expected to form hollow hydrogel structures.

The successful achievement of hollow hydrogels encourage us to explore the application as hydrogel-based pneumatic

DOI: 10.1021/acsami.9b17440
ACS Appl. Mater. Interfaces 2019, 11, 48564−48573

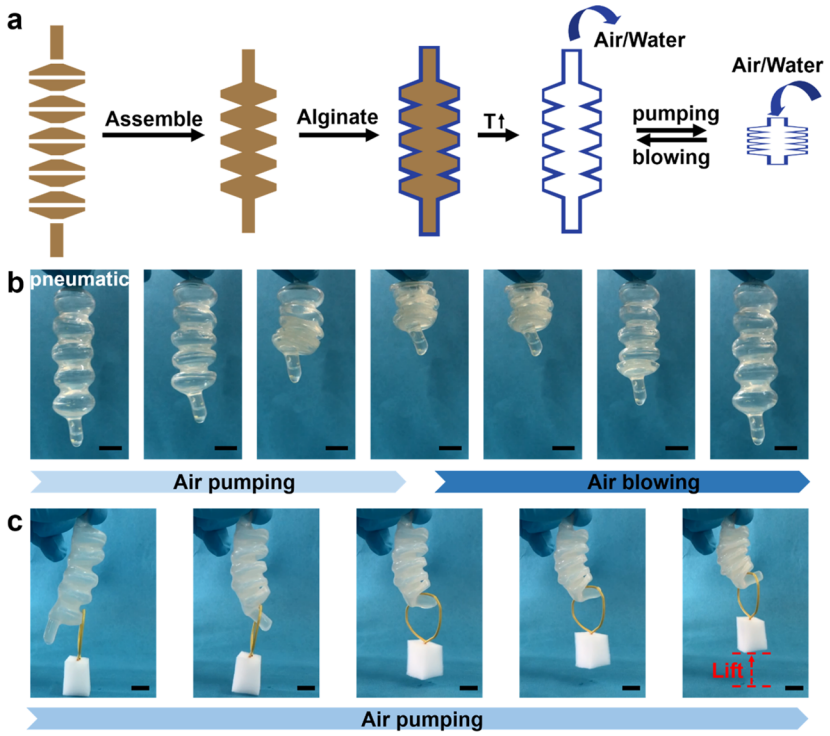

Figure 4. (a) Illustration and images showing the preparation of a telescopic pneumatic actuator. (b) Images showing the actuating and recovering process of pneumatic actuator and hydraulic actuator. (c) Images showing the process of lifting an object by an anisotropic pneumatic actuator. Scale bar: 1 cm.

actuators. As shown in Figure 4a, at first, two cylindrical gelatin cores and 10 disc-shaped gelatin cores were assembled together. After hydrogel growth and enucleated, a pneumatic actuator was obtained. The pneumatic actuator could be contracted and stretched alternatively by air pumping and air blowing (Figure 4b and Movie S5). Inspired by the opening process of the shell, the pneumatic actuator was installed into a shell that was made by paper. When air blowing, the pneumatic actuator would be stretched and the paper shell would be opened. Conversely, when air pumping, the pneumatic actuator would be contracted and the paper shell would be closed (Figure S17). The pneumatic actuator could turn to a hydraulic actuator by replacing the air with liquid (Figure S18 and Movie S6). Furthermore, two cylindrical gelatin cores and 10 inclined disc-shaped gelatin cores were assembled together, and an anisotropic pneumatic actuator was fabricated (Figure S19). It would bend when air is pumped, and it is considered as a mechanical gripper, which could lift an object during the pumping process and release it during the blowing process (Figure 4c and Movie S7).

It is well known that the blood vessels are typical hollow structures in living organisms, and blood could flow through the vessels efficiently. Single tubular-like and vascular-like channels have been fabricated and liquids could be smoothly transported through the hollow hydrogels (Figure S20 and Movies S8−10). The main functions of blood vessels are that nutrients are transported through it and delivered to tissue cells. Similarly, biological wastes are also passed on to the blood vessels and excluded from the body. Inspired by the function of blood vessels, the alginate hollow hydrogels are explored as material transport devices. The microstructures of the hollow hydrogel tube was investigated by scanning electron microscopy (SEM), as shown in Figure 5a, the internal surface of the hydrogel tunnel is much denser than the external surfaces due to Ca^{2+} diffused from the inside out, and there are connected holes in the tubular wall, the porous structures of the hydrogel make it possible to be used as microchannels. To test whether molecules could pass through the hydrogel layer, three electronegative dyes, tartrazine (M_w = 534.36), methyl blue (M_w = 799.80), Evans blue (M_w = 960.81) with the same concentration have been stored into a hydrogel container, respectively. The UV spectra of the outside solution have been measured as a function of time, and the concentration of the dyes outside the hydrogel container has been calculated (Figures S21−23). As shown in Figure 5b, the concentrations of all the three dyes outside the hydrogel container show an increasing tendency with increasing time, and the pass-through capacity is related to the molecular weight. Tartrazine, which has the lowest molecular weight among the three dyes, could effectively diffuse to the outside of the hydrogel container, while the penetration speed of Evans blue is very low. It could be speculated that if the molecular weight of a substance is high enough, it would be trapped in the hydrogel container. Since there are abundant carboxyl groups in the alginate chains, the alginate hydrogel walls will carry lots of negative charges as a result, therefore, the diffuse ability of molecules with opposite charges through the hydrogel layer will be different. Two model molecules, tartrazine, and methyl violet, with opposite charges and similar molecular weight have been investigated. As shown in Figure 5c, the one with negative charges will pass through the hydrogel wall effectively, and the positively charged dye shows a lower penetration speed, probably due to the complexation with the negative hydrogel wall (Figure S24).

In many chemical reactions, reactants are often required to slowly drip into the reaction flask. The process of molecular

DOI: 10.1021/acsami.9b17440
ACS Appl. Mater. Interfaces 2019, 11, 48564−48573

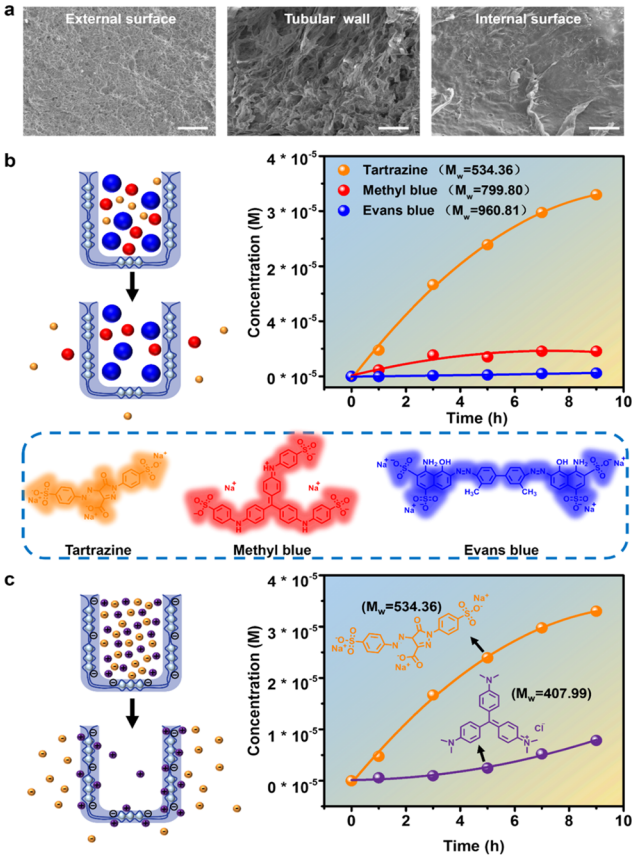

Figure 5. (a) External and internal surfaces of the hydrogel tube, and the cross-section SEM image of the tubular wall. (b) The diffusion performance of molecules with different molecular weight (tartrazine (M_w = 534.36), methyl blue (M_w = 799.80), Evans blue (M_w = 960.81)). (c) The diffusion performance of molecules with different charges (tartrazine (negative charges, M_w = 534.36), methyl violet (positive charges, M_w = 407.99)). Scale bar: 100 μm.

diffusion from the hydrogel tube is so slow, and it encourages us to explore the hollow hydrogels as reaction containers. As shown in Figure 6a,b, polyaniline (PANI) solution was stored into a hydrogel flask, and the hydrogel flask was immersed into alkaline condition. Because OH^- will diffuse into the hydrogel flask and PANI would be deprotonated in alkaline conditions and the color of the solution would gradually change from green to blue-violet. This demonstration provides an example to regulate the reaction speed, which may have potential applications in some circumstances that the reactants are not suitable for direct mixing. Moreover, reactions could also occur on the hydrogel wall. An alginate/PANI tubular hydrogel was prepared. When NaOH solution (0.1 M) flows through the alginate/PANI tubular hydrogel, the color of the tube would turn to blue-violet (Figure 6c,d and Movie S11), which makes it a promising candidate to detect the pH of the liquid pass through.

In addition, Au nanoparticles were fabricated on the internal surface of the hydrogel wall. As shown in Figure 7a, the hydrogel tube was first filled with dopamine solution, and dopamine will polymerize slowly into polydopamine and attached it to the inner wall of the tube. Then, the dopamine solution was changed by chloroauric acid solution. Because of the reductive property of catechol groups in the polydopamine layer, $AuCl_4^-$ ions will be reduced into Au atom, and finally, Au nanoparticles (AuNPs) will grow and anchor on the internal surface of hydrogel tube. SEM was applied to observe the appearance of the inner and outer walls of the hydrogel tube (Figure 7b). It can be obviously observed that a lot of bright and small particles appear on the inner wall of the tube, while nothing on the outer wall of the tube. Due to the remarkable catalytic properties of Au nanoparticles, the AuNPs containing hollow hydrogel could also be applied as a reaction container with catalytic ability. As shown in Figure 7c, a mixture solution of p-nitrophenol (2.5 mM) and sodium borohydride ($NaBH_4$, 0.25 M) was placed into the AuNPs modified alginate container, after 10 min, the solution changes from light yellow to colorless since p-nitrophenol is reduced to p-aminophenol due to the catalysis of AuNPs.

4. CONCLUSIONS

In summary, we have presented a novel and effective strategy to fabricate complex 3D hollow hydrogels with shape diversity,

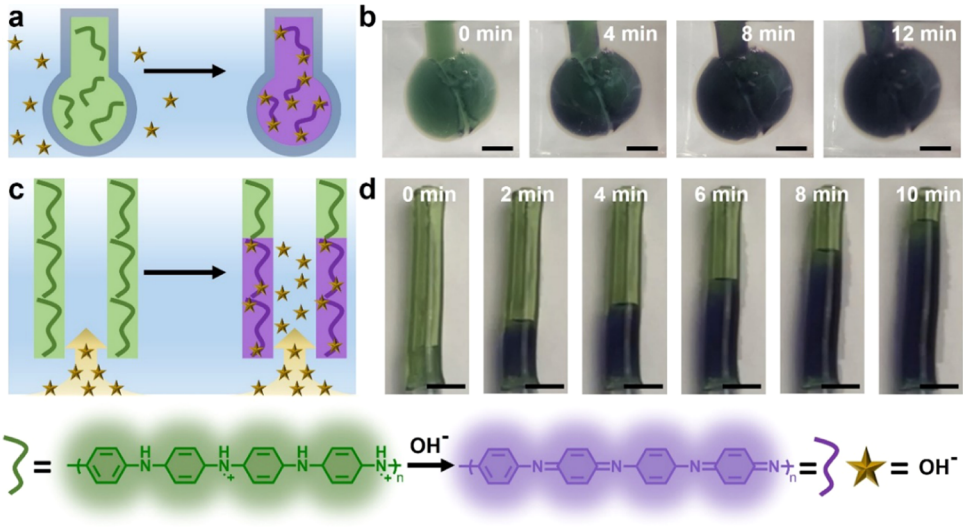

Figure 6. (a, b) Illustration and images show the process of OH- diffusion and conversion of oxidation and reduction states of polyaniline. (c, d) Illustration and images show the visual detection of pH in the flow channel. Scale bar: 1 cm.

DOI: 10.1021/acsami.9b17440
ACS Appl. Mater. Interfaces 2019, 11, 48564−48573

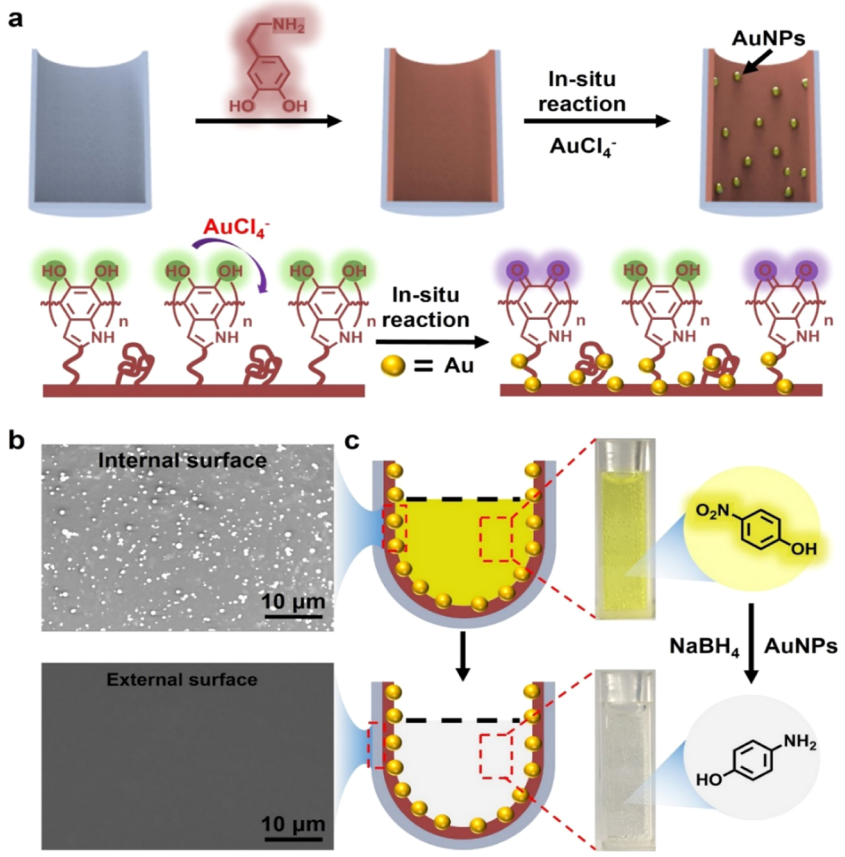

Figure 7. (a) Illustration showing the mechanism of in situ synthesis of AuNPs on the internal surface of hydrogel tube. (b) SEM images of the internal and external surfaces of the hydrogel tube, (c) illustration and images showing the solution of p-nitrophenol before and after being stored in the AuNPs modified alginate hydrogel container for 10 min. Scale bar: 1 cm.

and the obtained heterogeneous hollow hydrogels have various applications including material transportation and functional reaction containers. An assembled gelatin core loaded with Ca^{2+} was utilized to generate gelatin/alginate core−shell hydrogels through Ca^{2+}-alginate coordination, and alginate-based hollow hydrogels were further obtained by dissolving the gelation core in warm water. The thickness of the hydrogel layers could be tuned by adjusting the growth time or the cation species. Various 3D hollow structures could be achieved by starting with assembled gelatin cores and controlling the metal coordination position and strength. The obtained hollow hydrogels could be used as pneumatic/hydraulic actuators. Moreover, the capacity that could allow small molecules to pass through render the alginate hollow hydrogels ideal candidates for matter transportation, and reaction containers that could regulate the reaction speed have been demonstrated. In addition, functional polymers or nanoparticles have been introduced into the hydrogel wall, and functional hollow hydrogels have been developed. This work will inspire the design of novel complex hollow systems with great potential in various areas, including soft actuators, smart containers, etc.

■ ASSOCIATED CONTENT

Supporting Information

The Supporting Information is available free of charge at https://pubs.acs.org/doi/10.1021/acsami.9b17440.

Microscopic images of the hydrogel growth process; SEM images of hydrogel tubes, images of complex hollow hydrogels; preparation and actuating process of hydraulic/pneumatic actuator; process of molecule transportation and diffusion (PDF).

Process of air pumping and air blowing, the actuating process of hydraulic/pneumatic actuator, the liquid transportation process (Movie S1) (AVI)

Hollow hydrogel could be expanded when inhaling (Movie S2) (AVI)

Hollow hydrogel could be expanded when inhaling (Movie S3) (AVI)

Hollow hydrogel could be expanded when inhaling (Movie S4) (AVI)

Pneumatic actuator could be contracted and stretched alternatively by air pumping and air blowing (Movie S5) (AVI)

Pneumatic actuator would be contracted and the paper shell would be closed (Movie S6) (AVI)

Hydrogels bend when air is pumped, indicates it could lift an object during the pumping process and release it during the blowing process (Movie S7) (AVI)

Tubular-like and vascular-like channels have been fabricated, liquids could be smoothly transported through the hollow hydrogels (Movie S8) (AVI)

Liquids could be smoothly transported through the hollow hydrogels (Movie S9) (AVI)

Liquids could be smoothly transported through the hollow hydrogels (Movie S10) (AVI)

When NaOH solution (0.1 M) flows through the alginate/PANI tubular hydrogel, the color of the tube would turn to blue-violet (Movie S11) (AVI)

DOI: 10.1021/acsami.9b17440
ACS Appl. Mater. Interfaces 2019, 11, 48564−48573

AUTHOR INFORMATION

Corresponding Authors

*E-mail: zhangjiawei@nimte.ac.cn (J.Z.).
*E-mail: tao.chen@nimte.ac.cn (T.C.).

ORCID

Wei Lu: 0000-0002-2803-9519
Jiawei Zhang: 0000-0002-3182-9239
Afang Zhang: 0000-0002-0078-3223
Chih-Feng Huang: 0000-0002-8062-8708
Tao Chen: 0000-0001-9704-9545

Notes

The authors declare no competing financial interest.

ACKNOWLEDGMENTS

This work was supported by the National Key Research and Development Program of China (2018YFB1105100), the National Natural Science Foundation of China (51873223, 51773215, 21774138), Key Research Program of Frontier Science, Chinese Academy of Sciences (QYZDB-SSW-SLH036), the Natural Science Foundation of Ningbo (2018A610035), Youth Innovation Promotion Association of Chinese Academy of Sciences (2017337, 2019297), and Ningbo Science and Technology Bureau (2016C50009).

REFERENCES

(1) Zhao, N.; Wang, Z.; Cai, C.; Shen, H.; Liang, F. Y.; Wang, D.; Wang, C.; Zhu, T.; Guo, J.; Wang, Y. X.; Liu, X. F.; Duan, C. T.; Wang, H.; Mao, Y. Z.; Jia, X.; Dong, H. X.; Zhang, X. L.; Xu, J. Bioinspired Materials: from Low to High Dimensional Structure. *Adv. Mater.* **2014**, *26*, 6994−7017.

(2) Zhang, P. C.; Lin, L.; Zang, D. M.; Guo, X. L.; Liu, M. J. Designing Bioinspired Anti-Biofouling Surfaces Based on a Superwettability Strategy. *Small* **2017**, *13*, 1503334−1503343.

(3) Xue, L. J.; Kovalev, A.; Eichler-Volf, A.; Steinhart, M.; Gorb, S. N. Humidity-Enhanced Wet Adhesion on Insect-Inspired Fibrillar Adhesive Pads. *Nat. Commun.* **2015**, *6*, No. 6621.

(4) Kempaiah, R.; Nie, Z. H. From Nature to Synthetic Systems: Shape Transformation in Soft Materials. *J. Mater. Chem. B* **2014**, *2*, 2357−2368.

(5) Matsuda, T.; Kawakami, R.; Namba, R.; Nakajima, T.; Gong, J. P. Mechanoresponsive Self-Growing Hydrogels Inspired by Muscle Training. *Science* **2019**, *363*, 504−508.

(6) Rao, P.; Lin, T.; Chen, L.; Takahashi, R.; Shinohara, G.; Guo, H.; King, D. R.; Kurokawa, T.; Gong, J. P. Tough Hydrogels with Fast, Strong, and Reversible Underwater Adhesion Based on a Multiscale Design. *Adv. Mater.* **2018**, *30*, 1801884−1801892.

(7) Gan, D. L.; Xing, W. S.; Jiang, L. L.; Fang, J.; Zhao, C. C.; Ren, F. Z.; Fang, L. M.; Wang, K. F.; Lu, X. Plant-Inspired Adhesive and Tough Hydrogel Based on Ag-Lignin Nanoparticles-Triggered Dynamic Redox Catechol Chemistry. *Nat. Commun.* **2019**, *10*, No. 1487.

(8) Wu, B. Y.; Xu, Y. W.; Le, X. X.; Jian, Y. K.; Lu, W.; Zhang, J. W.; Chen, T. Smart Hydrogel Actuators Assembled via Dynamic Boronic Ester Bonds. *Acta Polym. Sin.* **2019**, *50*, 496−504.

(9) Zhao, Z.; Fang, R. C.; Rong, Q. F.; Liu, M. J. Bioinspired Nanocomposite Hydrogels with Highly Ordered Structures. *Adv. Mater.* **2017**, *29*, No. 1703045.

(10) Ko, H.; Javey, A. Smart Actuators and Adhesives for Reconfigurable Matter. *Acc. Chem. Res.* **2017**, *50*, 691−702.

(11) Wei, S. X.; Lu, W.; Le, X. X.; Ma, C. X.; Lin, H.; Wu, B. Y.; Zhang, J. W.; Theato, P.; Chen, T. Bioinspired Synergistic Fluorescence-Color-Switchable Polymeric Hydrogel Actuators. *Angew. Chem., Int. Ed.* **2019**, *58*, 16243−16251.

(12) Chen, D.; Zhang, Y.; Ni, C.; Ma, C.; Yin, J.; Bai, H.; Luo, Y.; Huang, F.; Xie, T.; Zhao, Q. Drilling by Light: Ice-Templated Photo-Patterning Enabled by a Dynamically Crosslinked Hydrogel. *Mater. Horiz.* **2019**, *6*, 1013−1019.

(13) Zhao, L.; Huang, J.; Zhang, Y.; Wang, T.; Sun, W.; Tong, Z. Programmable and Bidirectional Bending of Soft Actuators Based on Janus Structure with Sticky Tough PAA-Clay Hydrogel. *ACS Appl. Mater. Interfaces* **2017**, *9*, 11866−11873.

(14) Wang, Y. J.; Zhang, X. N.; Song, Y. P.; Zhao, Y.; Chen, L.; Su, F.; Li, L. B.; Wu, Z. L.; Zheng, Q. Ultrastiff and Tough Supramolecular Hydrogels with a Dense and Robust Hydrogen Bond Network. *Chem. Mater.* **2019**, *31*, 1430−1440.

(15) Huang, L. M.; Jiang, R. Q.; Wu, J. J.; Song, J. Z.; Bai, H.; Li, B.; Zhao, Q.; Xie, T. Ultrafast Digital Printing Toward 4D Shape Changing Materials. *Adv. Mater.* **2017**, *29*, No. 1605390.

(16) Liao, M. H.; Wan, P. B.; Wen, J. R.; Gong, M.; Wu, X. X.; Wang, Y. G.; Shi, R.; Zhang, L. Q. Wearable, Healable, and Adhesive Epidermal Sensors Assembled from Mussel-Inspired Conductive Hybrid Hydrogel Framework. *Adv. Funct. Mater.* **2017**, *27*, No. 1703852.

(17) Zhang, Y. C.; Liao, J. X.; Wang, T.; Sun, W. X.; Tong, Z. Polyampholyte Hydrogels with pH Modulated Shape Memory and Spontaneous Actuation. *Adv. Funct. Mater.* **2018**, *28*, No. 1707245.

(18) Li, X.; Cai, X. B.; Gao, Y. F.; Serpe, M. J. Reversible Bidirectional Bending of Hydrogel-Based Bilayer Actuators. *J. Mater. Chem. B* **2017**, *5*, 2804−2812.

(19) Chen, H.; Liu, Y. L.; Ren, B. P.; Zhang, Y. X.; Ma, J.; Xu, L. J.; Chen, Q.; Zheng, J. Super Bulk and Interfacial Toughness of Physically Crosslinked Double-Network Hydrogels. *Adv. Funct. Mater.* **2017**, *27*, No. 1703086.

(20) Long, T. J.; Li, Y. X.; Fang, X.; Sun, J. Q. Salt-Mediated Polyampholyte Hydrogels with High Mechanical Strength, Excellent Self-Healing Property, and Satisfactory Electrical Conductivity. *Adv. Funct. Mater.* **2018**, *28*, No. 1804416.

(21) Yao, L. J.; Li, Q.; Guan, Y.; Zhu, X. X.; Zhang, Y. J. Tetrahedral, Octahedral, and Triangular Dipyramidal Microgel Clusters with Thermosensitivity Fabricated from Binary Colloidal Crystals Template and Thiol−Ene Reaction. *ACS Macro Lett.* **2018**, *7*, 80−84.

(22) Liang, S. M.; Tu, Y. Q.; Chen, Q.; Jia, W.; Wang, W. H.; Zhang, L. D. Microscopic Hollow Hydrogel Springs, Necklaces and Ladders: a Tubular Robot as a Potential Vascular Scavenger. *Mater. Horiz.* **2019**, *6*, 2135−2142.

(23) Gao, Q.; He, Y.; Fu, J. Z.; Liu, A.; Ma, L. Coaxial Nozzle-Assisted 3D Bioprinting with Built-in Microchannels for Nutrients Delivery. *Biomaterials* **2015**, *61*, 203−216.

(24) Wu, W.; DeConinck, A.; Lewis, J. A. Omnidirectional Printing of 3D Microvascular Networks. *Adv. Mater.* **2011**, *23*, H178−H183.

(25) Hong, S.; Sycks, D.; Chan, H. F.; Lin, S.; Lopez, G. P.; Guilak, F.; Leong, K. W.; Zhao, X. H. 3D Printing of Highly Stretchable and Tough Hydrogels into Complex, Cellularized Structures. *Adv. Mater.* **2015**, *27*, 4035−4040.

(26) Chen, Z.; Zhao, D. H.; Liu, B. H.; Nian, G. D.; Li, X. K.; Yin, J.; Qu, S. X.; Yang, W. 3D Printing of Multifunctional Hydrogels. *Adv. Funct. Mater.* **2019**, *29*, No. 1900971.

(27) Ouyang, L. L.; Burdick, J. A.; Sun, W. Facile Biofabrication of Heterogeneous Multilayer Tubular Hydrogels by Fast Diffusion-Induced Gelation. *ACS Appl. Mater. Interfaces* **2018**, *10*, 12424−12430.

(28) He, M.; Zhao, Y. T.; Duan, J. J.; Wang, Z. G.; Chen, Y.; Zhang, L. N. Fast Contact of Solid−Liquid Interface Created High Strength Multi-Layered Cellulose Hydrogels with Controllable Size. *ACS Appl. Mater. Interfaces* **2014**, *6*, 1872−1878.

(29) Ma, S. H.; Yan, C. Y.; Cai, M. R.; Yang, J.; Wang, X. L.; Zhou, F.; Liu, W. M. Continuous Surface Polymerization via Fe (II)-Mediated Redox Reaction for Thick Hydrogel Coatings on Versatile Substrates. *Adv. Mater.* **2018**, *30*, 1803371−1803379.

(30) Ma, S. H.; Rong, M. M.; Lin, P.; Bao, M.; Xie, J.; Wang, X. L.; Huck, W. T. S.; Zhou, F.; Liu, W. M. Fabrication of 3D Tubular Hydrogel Materials Through On-Site Surface Free Radical Polymerization. *Chem. Mater.* **2018**, *30*, 6756−6768.

DOI: 10.1021/acsami.9b17440
ACS Appl. Mater. Interfaces 2019, 11, 48564−48573

(31) Lin, H. J.; Ma, S. H.; Yu, B.; Cai, M. R.; Zheng, Z. J.; Zhou, F.; Liu, W. M. Fabrication of Asymmetric Tubular Hydrogels Through Polymerization-Assisted Welding for Thermal Flow Actuated Artificial Muscles. *Chem. Mater.* **2019**, *31*, 4469−4478.
(32) Yan, X. Z.; Wang, F.; Zheng, B.; Huang, F. H. Stimuli-Responsive Supramolecular Polymeric Materials. *Chem. Soc. Rev.* **2012**, *41*, 6042−6065.
(33) Liu, K.; Kang, Y. T.; Wang, Z. Q.; Zhang, X. Reversible and Adaptive Functional Supramolecular Materials: "Noncovalent Interaction" Matters. *Adv. Mater.* **2013**, *25*, 5530−5548.
(34) Ma, C. X.; Li, T. F.; Zhao, Q.; Yang, X. X.; Wu, J. J.; Luo, Y. W.; Xie, T. Supramolecular Lego Assembly Towards Three-Dimensional Multi-Responsive Hydrogels. *Adv. Mater.* **2014**, *26*, 5665−5669.
(35) Ju, G.; Cheng, M.; Guo, F.; Zhang, Q.; Shi, F. Elasticity-Dependent Fast Underwater Adhesion Demonstrated by Macroscopic Supramolecular Assembly. *Angew. Chem., Int. Ed.* **2018**, *57*, 8963−8967.
(36) Cheng, M. J.; Zhu, G. Q.; Li, L.; Zhang, S.; Zhang, D. Q.; Kuehne, A. J. C.; Shi, F. Parallel and Precise Macroscopic Supramolecular Assembly Through Prolonged Marangoni Motion. *Angew. Chem., Int. Ed.* **2018**, *57*, 14106−14110.
(37) Zhang, Y. C.; Le, X. X.; Jian, Y. K.; Lu, W.; Zhang, J. W.; Chen, T. 3D Fluorescent Hydrogel Origami for Multistage Datan Security Protection. *Adv. Funct. Mater.* **2019**, *29*, No. 1905514.
(38) Ma, C. X.; Le, X. X.; Tang, X. L.; He, J.; Xiao, P.; Zheng, J.; Xiao, H.; Lu, W.; Zhang, J. W.; Huang, Y. J.; Chen, T. A Multiresponsive Anisotropic Hydrogel with Macroscopic 3D Complex Deformations. *Adv. Funct. Mater.* **2016**, *26*, 8670−8676.
(39) Le, X. X.; Lu, W.; Zheng, J.; Tong, D. Y.; Zhao, N.; Ma, C. X.; Xiao, H.; Zhang, J. W.; Huang, Y. J.; Chen, T. Stretchable Supramolecular Hydrogels with Triple Shape Memory Effect. *Chem. Sci.* **2016**, *7*, 6715−6720.
(40) Xiao, H.; Lu, W.; Le, X. X.; Ma, C. X.; Li, Z. W.; Zheng, J.; Zhang, J. W.; Huang, Y. J.; Chen, T. A Multi-Responsive Hydrogel with a Triple Shape Memory Effect Based on Reversible Switches. *Chem. Commun.* **2016**, *52*, 13292−13295.
(41) Lu, W.; Le, X. X.; Zhang, J. W.; Huang, Y. J.; Chen, T. Supramolecular Shape Memory Hydrogels: A New Bridge Between Stimuli-Responsive Polymers and Supramolecular chemistry. *Chem. Soc. Rev.* **2017**, *46*, 1284−1294.
(42) Wang, L.; Jian, Y. K.; Le, X. X.; Lu, W.; Ma, C. X.; Zhang, J. W.; Huang, Y. J.; Huang, C. F.; Chen, T. Actuating and Memorizing Bilayer Hydrogels for a Self-deformed Shape Memory Function. *Chem. Commun.* **2018**, *54*, 1229−1232.
(43) Ma, C. X.; Lu, W.; Yang, X. X.; He, J.; Le, X. X.; Wang, L.; Zhang, J. W.; Serpe, M. J.; Huang, Y. J.; Chen, T. Bioinspired Anisotropic Hydrogel Actuators With On−Off Switchable and Color-Tunable Fluorescence Behaviors. *Adv. Funct. Mater.* **2018**, *28*, No. 1704568.
(44) Le, X. X.; Lu, W.; Zhang, J. W.; Chen, T. Recent Progress in Biomimetic Anisotropic Hydrogel Actuators. *Adv. Sci.* **2019**, *6*, No. 1801584.
(45) Jian, Y. K.; Lu, W.; Zhang, J. W.; Chen, T. Research Progress in Supramolecular Shape Memory Hydrogels. *Acta Polymerica Sinica* **2018**, *11*, 1385−1399.
(46) Le, X. X.; Lu, W.; Xiao, H.; Wang, L.; Ma, C. X.; Zhang, J. W.; Huang, Y. J.; Chen, T. Fe^{3+} -, pH-, Thermoresponsive Supramolecular Hydrogel with Multishape Memory Effect. *ACS Appl. Mater. Interfaces* **2017**, *9*, 9038−9044.

DOI: 10.1021/acsami.9b17440
ACS Appl. Mater. Interfaces 2019, 11, 48564−48573